Atom-resolved observation of Na ensembles activating CO_2 adsorption on a $TiO_2(110)$-(1×1) surface as the genesis of basic sites

Hiroshi Onishi and Yasuhiro Iwasawa[1]

Department of Chemistry, Graduate School of Science, The University of Tokyo, Hongo, Bunkyo-ku, Tokyo 113, Japan

Received 29 September 1995; accepted 9 January 1996

We have succeeded in observing the structure-sensitive reaction of CO_2 with $TiO_2(110)$-(1×1) surfaces modified with Na adatoms by scanning tunneling microscopy. At low coverages (0.4 atom/nm^2 or less) Na adatoms are ionized and adsorbed on the exposed Ti-rows of the substrate. A p(4×2) order locally appears at 0.6 atom/nm^2, and a c(4×2) order develops at 0.9 atom/nm^2. Those Na-modified surfaces are exposed to 10^2 L CO_2 at room temperature. Post-exposure observation finds chains of bright particles on the c(4×2) surface. The asymmetric topography of the individual particles is assigned to the distribution of the LUMO of the adsorbed carbonate. In contrast, dispersed Na adatoms at lower coverages are unable to react with CO_2 at all. The genesis of strong basic sites is thus suggested not to be linearly correlated with Na quantity, but to be correlated with the ordered structure of Na adatoms.

Keywords: acid–base catalysis; alkali additives; scanning tunneling microscopy; carbon dioxide; titanium oxide

1. Introduction

Alkali additives in metal-oxide catalysts have extensively been attracting attention. The base strength of doped catalysts are so remarkably enhanced that they are often termed "super-base" [1,2]. Acid–base reactivity is one of the important properties of metal-oxide catalysts, and its control is of interest in surface chemistry as well as in industrial applications [3,4]. In addition, the oxidative coupling reaction of methane has been found to proceed on oxide catalysts promoted by alkali additives [5,6]. To consider how the alkali additives promote the basic character and activity of metal-oxide catalysts, we have already studied Na-deposited $TiO_2(110)$ single crystal surface by conventional photoelectron spectroscopic techniques [7]. Monolayer (ML) coverage was determined on a break observed in Na(1s) emission intensity plotted versus Na deposition time [7]. Chemisorption of CO_2, a typical acid–base reaction at surface, has further been tested to examine the reactivity of the modified surface [8]. XPS and UPS results have shown that submonolayer coverages of Na adatoms remarkably enhance the adsorption of carbon dioxide on the TiO_2 surface forming carbonate,

$$CO_2 + O_s^{2-} \rightarrow CO_3^{2-} \quad (1)$$

where O_s^{2-} represents an oxygen ion of the substrate. The enhanced adsorption is attributed to the promotion in the base strength of the oxygen ions by Na adatoms. The amount of carbonates thus formed varied with Na coverage exhibiting an S-shaped dependence, as shown in fig. 1 [8]. A critical coverage of 0.3 ML for carbonate formation coincided with the onset of a c(4×2) pattern in low energy electron diffraction (LEED), suggesting a strong structure-dependent character of the promotion.

In the present letter, we report the reaction of CO_2 with Na-promoted $TiO_2(110)$ surface of different Na coverages observed by scanning tunneling microscopy (STM). This is an atomic-scale observation of the mechanism producing structural sensitivity in a reaction on a metal/metal-oxide model catalyst.

Rutile TiO_2 formally comprises Ti^{4+} and O^{2-} ions. Each Ti^{4+} ion is coordinated to an octahedron of six O^{2-} ions in the bulk crystal [9]. A $TiO_2(110)$ surface prepared by argon ion sputtering and vacuum annealing exhibits a (1×1)-ordered structure. A stoichiometric model (fig. 2) is conceived for the (1×1) surface [10], where rows of Ti ions (Ti-rows) and ridges of O ions (O-ridges) are alternatively exposed. In recent STM studies [11–15] regular rows were found on the (1×1) surface and

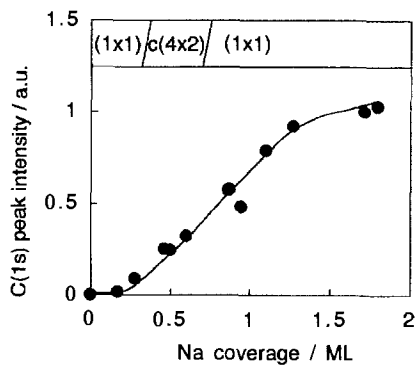

Fig. 1. The amount of adsorbed carbonate on the Na-modified $TiO_2(110)$ surface as a function of Na coverage [8].

[1] To whom correspondence should be addressed.

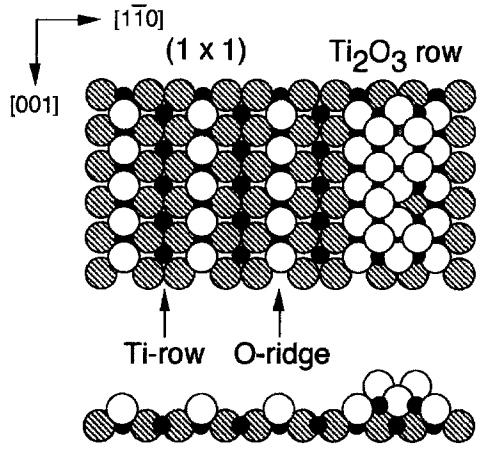

Fig. 2. Stoichiometric model for $TiO_2(110)$-(1 × 1) surface with a Ti_2O_3 added row. Small and large symbols represent Ti^{4+} and O^{2-} ions, respectively. An oxygen ion is removed from the added row for illustration. Top and side views are shown.

assigned to the exposed Ti-rows. In those STM studies also a protruding row-like species containing double strands was found. When the double-strand reconstruction covered the surface, a (1 × 2) pattern accordingly appeared in LEED. Quite recently, Murrey et al. have observed p(4 × 2)-ordered Na adatoms deposited on the $TiO_2(110)$-(1 × 2) surface by STM [16]. The interpretation of the double-strand topography on the reconstructed surface remains controversial: an added Ti_2O_3 row model (fig. 2) [12], and three types of missing-oxygen row models [11,14,17] have been proposed. An STM study of a DCOO-covered $TiO_2(110)$ surface [15], where Ti ions on the surface were titrated by imaging individual formate ions, revealed the absence of Ti ions exposed on the double-strand row. This gives strong evidence for the added Ti_2O_3 row model as a surface-limited phase of titanium oxide. In the present study on the unreconstructed $TiO_2(110)$-(1 × 1) substrate, we have resolved individual Na atoms in the c(4 × 2)-ordered adlayer responsible for the CO_2 adsorption.

2. Experimental

The experiments were performed in a scanning tunneling microscope (JSTM4500VT, JEOL) with a base pressure of 2×10^{-8} Pa. Constant current topography was observed with a Pt–Ir tip. A polished $TiO_2(110)$ wafer of $6.5 \times 1 \times 0.25$ mm^3 (Earth Chemicals) was cleaned with cycles of argon-ion sputtering (3 keV, 0.3 μA, 3 min) and vacuum annealing at 900 K [12,15]. An IR radiation thermometer (IR-FBP, Chino) monitored surface temperature. The annealed crystal became deep blue and gave a (1 × 1) LEED pattern. An oxygen deficiency of 0.001% was estimated from electrical resistivity of the crystal [18]. Sodium atoms were deposited with a dispenser source (Saes Getters) resistively heated in the microscope. Sodium dosage was controlled by deposition time. Sodium deposition, CO_2 exposure, and STM observation were done on the (1 × 1) surface cooled for 1 h after the annealing. Surface temperature of the cooled crystal was below the lower limit of the thermometer and estimated to be 300–350 K.

3. Results and discussion

3.1. Deposited Na adatoms

Fig. 3 shows constant current topography of Na adatoms deposited on a $TiO_2(110)$-(1 × 1) surface. Regular rows of contrast on the clean surface, shown in fig. 3a, have been assigned to the exposed Ti-rows along the [001] direction [12,15]. Individual Ti ions were resolved as axial corrugations on the rows. When the substrate was exposed to the Na flux for 90 s, bright spots of 0.1 nm height randomly appeared *on* the Ti-rows. Sodium coverage of the surface in fig. 3b corresponded to 0.1 ML in the scale of fig. 1. Forty one spots were counted in fig. 3b. The number of spots increased in proportion to deposition time. Hence, we assume that a spot represents a Na adatom. The absolute coverage of Na at the surface in fig. 3b was 0.2 atom/nm^2 on this assumption. The dispersed geometry in the dilute adlayer indicates repulsive force between the adatoms. The electrostatic repulsion among ionized adatoms is responsible for the structure. Indeed, an oxidation shift of 0.9 eV in Na(1s) XPS emission demonstrated that Na adatoms of 0.1 ML were ionized to the Na^+ state [7]. The resultant electron transport from the adatoms to the substrate caused a substantial decrease in work function of the Na-modified surface [7].

A p(4 × 2) order was locally formed on the surface exposed to the Na flux for 420 s. A rectangular lattice of the p(4 × 2) order was observed at the center of fig. 3c, where Na coverage was determined as 0.6 atom/nm^2 based on the surface density of imaged particle. This p(4 × 2) order did not develop over the surface being replaced by the c(4 × 2) order at higher coverages. The instability of the p(4 × 2)-ordered ensemble is consistent with the absence of the according pattern in LEED observation [7]. A similar p(4 × 2)-ordering of Na adatoms has been observed on a (1 × 2)-reconstructed $TiO_2(110)$ surface [16]. Fig. 3d shows a nearly completed c(4 × 2)-ordered overlayer of 0.9 Na atom/nm^2. The structure of these dense overlayers fluctuated even at room temperature. A model for the ordered structures is illustrated in fig. 4. We assume in the model that a bright spot in the images represents a Na adatom adsorbed on a Ti-row, though the Ti-row could not be resolved under the dense Na-layers shown in figs. 3c and 3d. Thus, our previous model for the c(4 × 2) surface [7,8] should be revised on the results by STM. We may have failed in the accurate estimation of analyzer transmission character-

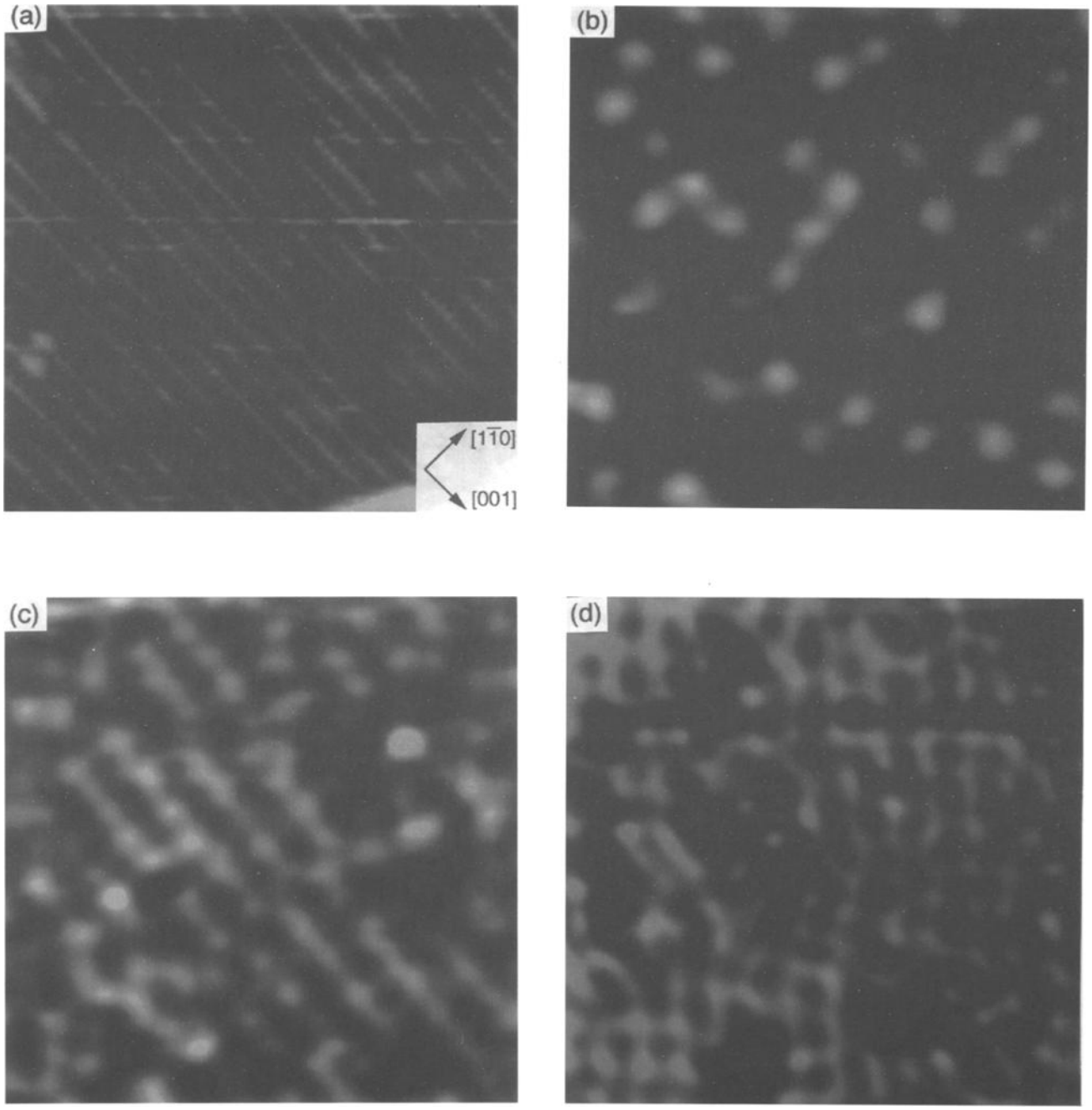

Fig. 3. Constant current topography (14×14 nm^2) of Na-modified TiO_2(110)-(1×1) surfaces. (a) Clean surface (sample bias voltage $V_s = +1.0$ V, tunneling current $I_t = 0.3$ nA), (b) dispersed Na adatoms ($V_s = +2.0$ V, $I_t = 0.1$ nA), (c) p(4×2)-ordered surface ($V_s = +2.0$ V, $I_t = 0.3$nA), and (d) c(4×2)-ordered surface ($V_s = -2.0$ V, $I_t = 0.5$ nA).

istics in XPS analysis, and overestimated the absolute density of Na in our previous reports [7,8].

The minimal distance between Na adatoms is 1.18 and 0.88 nm in the p(4×2) and c(4×2) models, respectively. The values are much larger than the nearest neighbor distance in Na bcc metal, 0.37 nm. A (110) truncation of a Na crystal is compared in the same scale in fig. 4. This suggests that Na adatoms are non-metallic in the ordered layers. Indeed, a scanning tunneling spectroscopy (STS) measurement found a gap of 1.6 V in the band structure of the c(4×2) surface, proving non-metallic states of the adatoms. On the other hand, the ionic charge of the adatoms reduces with Na coverage due to destabilization by the electrostatic repulsion, as demonstrated by a shift in the binding energy of Na(1s) emission [7]. The Na adatoms on the c(4×2) surface are incompletely ionized to $Na^{\delta+}$ ($\delta < 1$), and the direct interaction of these adatoms is too weak to build a metallic band structure. The reactivity of Na adatoms in two different phases, the c(4×2) structure comprising $Na^{\delta+}$

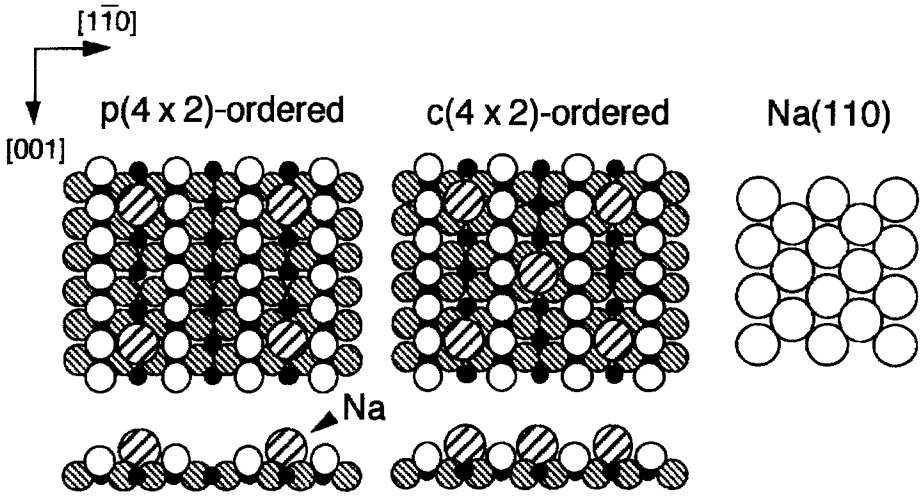

Fig. 4. Models for p(4 × 2)-Na and c(4 × 2)-Na adlayers deposited on the $TiO_2(110)$-(1 × 1) surface. A (110) truncation of a Na crystal is also shown in the same scale.

atoms vs. randomly dispersed Na^+, is compared in the following section.

3.2. *Reaction with CO_2*

The $Na^{\delta+}$ adatoms in the c(4 × 2) surface were reactive to CO_2. Fig. 5a shows the topography observed on a c(4 × 2) surface exposed to 10^2 L CO_2 at the ambient temperature. The c(4 × 2) order disappeared and chains of spots appeared along the [001] direction. The chains were locally ordered in a p(3×2) symmetry. In contrast to the reaction on the c(4 × 2) surface, CO_2 was not adsorbed on a surface with randomly dispersed Na^+ ions at all. Dispersed Na ions remain unchanged on the surface after the exposure to 10^2 L CO_2, as shown in fig. 5b. The absence of reactivity of the surface modified with dispersed Na ions is consistent with the threshold observed in fig. 1 [8].

Individual spots observed on the CO_2-exposed c(4 × 2) surface gave rise to an asymmetric topography elongated in the [1$\bar{1}$0] direction. The asymmetry reflects the intra-molecular structure of the imaged species. A single atom of neither Na, Ti, nor O is responsible for the asymmetric topography. We assign the observed spots to the carbonate ions produced in reaction (1), as characterized by XPS and UPS [8]. A CO_2 molecule adsorbed

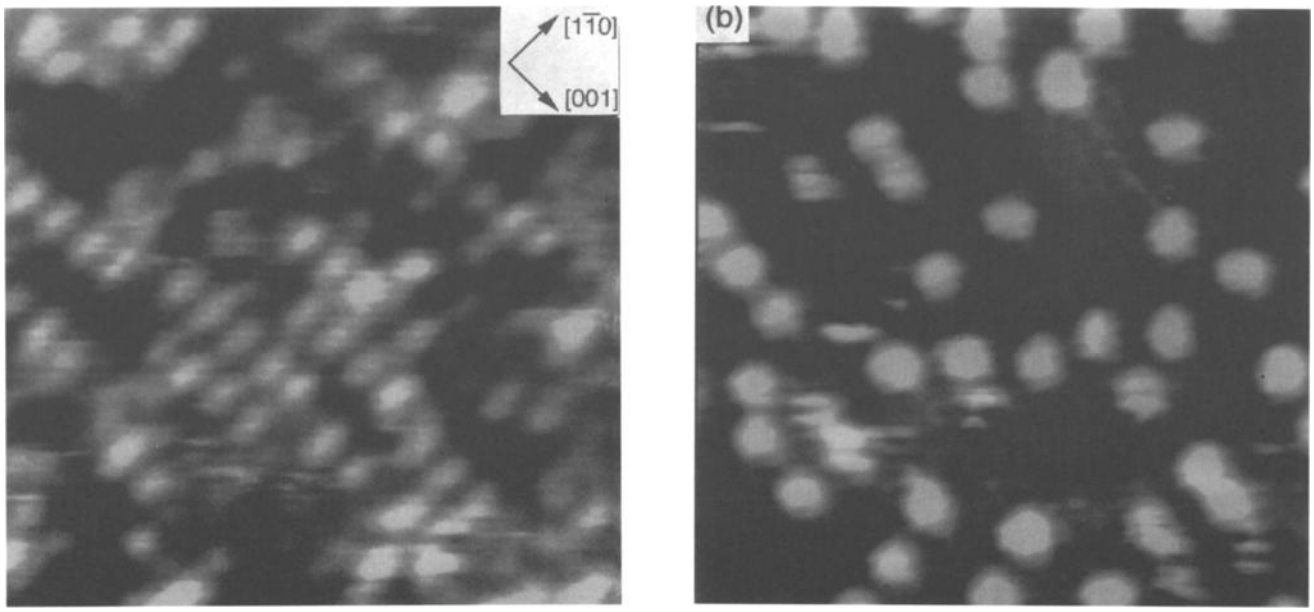

Fig. 5. Constant current topography (20 × 20 nm^2) of Na-modified $TiO_2(110)$-(1 × 1) surfaces exposed to 10^2 L CO_2. (a) Carbonate chains formed on a c(4 × 2)-Na surface ($V_s = +2.0$ V, $I_t = 0.1$ nA), and (b) a dispersed-Na adlayer ($V_s = +2.0$ V, $I_t = 0.1$ nA).

at the on-top site of an O^{2-} ion in the O-ridge yields a carbonate ion, CO_3^{2-}, as illustrated in fig. 6a. The observed topography is reproduced by tunneling to the lowest unoccupied molecular orbital (LUMO) of the carbonate ion. The image in fig. 5a was observed with a positive sample bias voltage of 2.0 V, being generated by tunneling to vacant states on the surface. Tunneling from occupied states could not be observed, because reversing the bias polarity led to an unstable tunneling junction. The LUMO of a free carbonate ion, $2a_2''$, is an anti-bonding π^* combination of $2p_z$ orbitals of the carbon and three oxygen atoms in the carbonate ion [19]. Assuming the on-top geometry, the distribution of the LUMO along the lifted O–C–O bonding reproduces the observed topography of the spots, as illustrated in fig. 6b. Na adatoms are located between the adsorbed CO_2 and the substrate in the model of fig. 6a, to stabilize the large and poorly-coordinated carbonate ions. It is interesting that the adsorbed carbonate ions form chains. Carbonate ions form a similar one-dimensional array in the bulk crystal of $Na_2CO \cdot H_2O$ [20].

Finally, it is considered how Na ensembles on the c(4 × 2) surface promote the reaction of CO_2 molecules with the TiO_2 substrate. The formation of a CO_2^- radical anion is known on polycrystalline Na-film [21], Na-deposited Pd(111) [22], K-deposited Pt(111) [23], and K-deposited Pd(100) [24] surfaces. On those surfaces, alkali atoms in metallic states give an electron to a CO_2 molecule to yield a CO_2^- ion,

$$CO_2 + \text{alkali metal} \rightarrow CO_2^- \quad (2)$$

We assume a similar CO_2^--mediated mechanism on the c(4 × 2)-Na surface; electron attachment to an impinging CO_2 molecule, reaction (2), takes place at the incompletely ionized $Na^{\delta+}$ adatoms on the c(4 × 2) surface. The postulated CO_2^- radical intermediates can be immediately trapped by the oxygen ions in the protruding O-ridges to form the carbonate ions. Highly ionized Na^+ adatoms in the dispersed phase are unable to transfer their valence electron to CO_2. The atomic-scale structure of Na ensembles dominates the energy position and electron population of the ionized states localized on the individual Na adatoms, since the electrostatic repulsion strongly depends on adatom–adatom distance.

Two CO_2^- ions might couple to an oxalate ion, $C_2O_4^{2-}$, and then disproportionate to a carbonate ion and a CO molecule, as reported on poly-Na [21], K/Pt(111) [23] and K/Pd(100) [24] surfaces and also in inert gas matrices containing Li atoms [25]:

$$2CO_2^- \rightarrow C_2O_4^{2-} \quad (3)$$

$$C_2O_4^{2-} \rightarrow CO_3^{2-} + CO\uparrow \quad (4)$$

The coupling and disproportionation reactions were not observed on the c(4 × 2)-Na surface. No CO production was detected during CO_2 exposure in gas phase analysis by a mass spectrometer. The coupling product, oxalate ion, was not detected on the CO_2-exposed surfaces by XPS and UPS [8].

In summary, we have visualized the mechanism producing structural sensitivity in the reaction of CO_2 with Na-modified TiO_2(110) model catalyst by atom-resolved STM observation. Ionized Na adatoms are randomly adsorbed on the exposed Ti-rows of the substrate at a low coverage (0.4 atom/nm^2) . A p(4 × 2) order locally appears at 0.6 atom/nm^2, and a c(4 × 2) order develops at 0.9 atom/nm^2. Ordered carbonate ions are observed as asymmetric particles on the c(4 × 2)-Na surface upon CO_2 exposure, whereas dispersed Na adatoms at lower coverages are unable to react with CO_2. A CO_2^--mediated mechanism is assumed for the reaction. The genesis of strong basic sites is thus demonstrated not

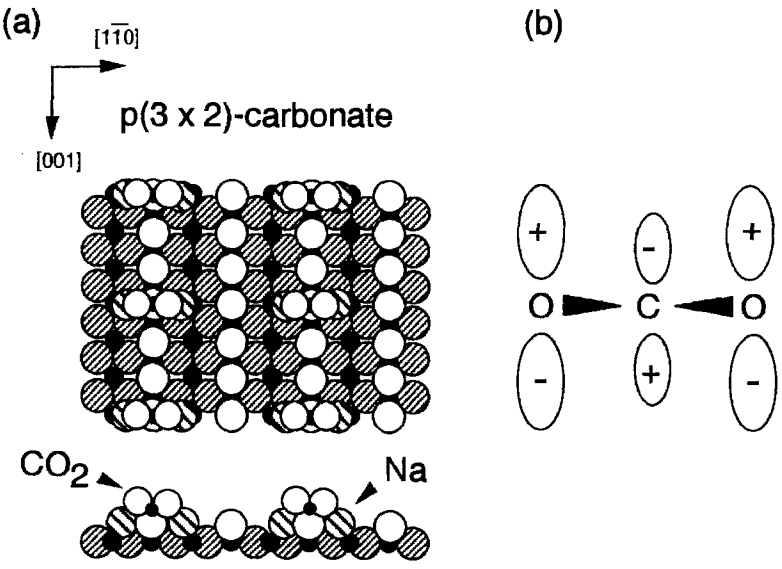

Fig. 6. Model for the p(3 × 2)-ordered carbonate ions formed on the CO_2-exposed c(4 × 2)-Na surface. (a) Geometry of the p(3 × 2)-ordered carbonate ions, and (b) on-top view of the LUMO of the adsorbed carbonate ion.

to be linearly correlated with Na quantity, but to be correlated with the atomic-scale structure of Na ensembles.

References

[1] J. Kijenski and S. Marinowski, Bull. Acad. Polon. Sci. 25 (1977) 428.
[2] K. Tanabe, in: *Catalysis by Acids and Bases*, eds. B. Imelik, C. Naccache, G. Coudurier, Y. Ben Taarit and J.C. Vedrine (Elsevier, Amsterdam, 1984) p. 1.
[3] K.Tanabe, *Solid Acids and Bases* (Academic Press, New York, 1970).
[4] H.A. Benesi and B.H.C. Winquist, Adv. Catal. 27 (1978) 97.
[5] C.-H. Lin, J.-X. Wang and J.H. Lunsford, J. Catal. 111 (1988) 302.
[6] Z. Zhang, X.E. Verykios and M. Baerns, Catal. Rev. 36 (1994) 507.
[7] H. Onishi, T. Aruga, C. Egawa and Y. Iwasawa, Surf. Sci. 199 (1988) 54.
[8] H. Onishi, T. Aruga, C. Egawa and Y. Iwasawa, J. Chem. Soc. Faraday Trans. I 85 (1989) 2597.
[9] R.W.G. Wyckoff, in: *Crystal Structure*, Vol. 1, 2nd Ed. (Wiley, New York, 1965) p. 251.
[10] V.E. Henrich and P.A. Cox, *The Surface Science of Metal Oxides* (Cambridge University Press, Cambridge, 1994).
[11] M. Sander and T. Engel, Surf. Sci. 302 (1994) L263.
[12] H. Onishi and Y. Iwasawa, Surf. Sci. 313 (1994) L783.
[13] D. Novak, E. Garfunkel and T. Gustafsson, Phys. Rev. B 50 (1994) 5000.
[14] P.W. Murrey, N.G. Condon and G. Thornton, Phys. Rev. B 51 (1995) 10989.
[15] H. Onishi, K. Fukui and Y. Iwasawa, Bull. Chem. Soc. Jpn. 68 (1995) 2447.
[16] P.W. Murrey, N.G. Condon and G. Thornton, Surf. Sci. 323 (1995) L281.
[17] P.J. Møller and M.-C. Wu, Surf. Sci. 224 (1989) 265.
[18] H. Onishi and Y. Iwasawa, Jpn. J. Appl. Phys. 33 (1994) L1338.
[19] J.A. Tossel, J. Phys. Chem. Solids 37 (1976) 1043.
[20] R.W.G. Wyckoff, in: *Crystal Structure*, Vol. 3, 2nd Ed. (Wiley, New York, 1965) p. 545.
[21] J. Paul, F.M. Hoffmann and J.L. Robbins, J. Phys. Chem. 92 (1988) 6967.
[22] S. Wohlrab, D. Ehrlich, J. Wambach, H. Kuhlenbeck and H.-J. Freund, Surf. Sci. 220 (1989) 243.
[23] Z.M. Liu, Y. Zhou, F. Solymosi and J.M. White, J. Phys. Chem. 93 (1989) 4383.
[24] F. Solymosi and A. Berkó, J. Catal. 101 (1986) 458.
[25] Z.H. Kafafi, R.H. Hauge, W.E. Billups and J.L. Margrave, J. Am. Chem. Soc. 105 (1983) 3886.